



# Larval dispersal from an energetic tidal channel and implications for blue mussel (*Mytilus edulis*) shellfisheries

Jonathan Demmer<sup>1</sup> · Simon P. Neill<sup>1</sup> · Olga Andres<sup>2</sup> · Shelagh K. Malham<sup>1</sup> · Trevor Jones<sup>3</sup> · Peter Robins<sup>1</sup>

Received: 4 November 2021 / Accepted: 23 July 2022 / Published online: 16 August 2022  
© The Author(s) 2022

## Abstract

Complex coastal currents control early-stage larval dispersal from intertidal populations, and late-stage settlement patterns, but are often poorly resolved in larval dispersal models. Generally, there is high uncertainty in the timing of larval spawning, which markedly affects larval dispersal. In this study, we describe the physical parameters that induce spawning events in the blue mussel, *Mytilus edulis*, using a variation of the Condition Index (which relates the mass of meat to the mass of the shell) as a proxy. We developed a high-resolution Eulerian coastal hydrodynamic model, coupled with a Lagrangian particle tracking model, to quantify the potential dispersal of early-stage mussel larvae based on differing spawning dates obtained from field data. Our results showed that (1) the timings of larval spawning cannot be explained solely by ‘thermal shocks’ in the sea or air temperatures (i.e. fluctuations in temperature causing stress); (2) larger spawning events generally occurred during neap tides; (3) the simulated larval dispersal was largely but not always predicted by averaged current pathways (calculated over two weeks period); and (4) simulated self-recruitment was low at sites associated with strong tidal currents. These results have important implications for shellfisheries stock management and sustainability. Specific to this study, simulated mussels from shellfishery beds off North Wales dispersed more than 25 km in one week and so could feasibly contribute to the wider population throughout the northern part of the Irish Sea.

**Keywords** Particle tracking · Tide · Larval dispersal · Modelling · Condition Index · Blue mussels

---

Handling Editor: Michael Hartnett

✉ Jonathan Demmer  
j.demmer@bangor.ac.uk

<sup>1</sup> School of Ocean Sciences, Bangor University, Menai Bridge, Askew Street, LL59 5AB, UK

<sup>2</sup> CEFAS, Pakefield Road, Lowestoft, Suffolk NR33 0HT, UK

<sup>3</sup> Extramussel Limited, Refail Llanffinan, Llangefni LL77 7SN, Anglesey, UK

## Introduction

Benthic marine organisms often spend their early life stages in the water column, where larvae are subjected to dispersal via ocean currents, mediated by species-specific biological traits. These *biophysical* interactions ultimately control population dynamics (i.e. connectivity and self-recruitment). Oscillatory tidal currents and persistent (baroclinic) density-driven flows, as well as coastal and wind-driven surface currents, have been shown to influence larval dispersal (e.g. Harnett et al. 2007; Rhörs et al. 2014). There is a lack of studies resolving the complexity of coastal currents on larval dispersal. The study by Dauhajre et al. (2019) on particles dispersed from the east coast of the USA showed the importance of high-resolution models to resolve complex coastal currents. However, that study described deep coastal currents with an upwelling system, which differs from relatively shallow, well-mixed environments such as those common in northwest Europe. The biological traits of larvae – the timing of spawning, their growth and metamorphosis rate, pelagic larval duration (PLD), vertical migration behaviour, mortality and settlement behaviour – will further influence their transport. These traits depend on individual fitness, food availability and temperature or salinity gradients (Troost et al. 2008; James et al. 2019). The relative importance of these physical and biological parameters on larval dispersal, population connectivity and self-recruitment varies over tidal, seasonal, inter-annual and climatic time scales, but also varies geographically and for different species (Sheaves 2009; Nanninga & Berumen 2014; James et al. 2019). Even over scales of tens of kilometres, mussel larvae can experience significantly different ocean currents, which will influence their self-recruitment and connectivity (Becker et al. 2007).

The blue mussel, *Mytilus edulis* Linnaeus (1758), is a sessile benthic bivalve, which can be found in the intertidal zone on any substratum providing a secure anchorage such as rocks, stones, gravels, shingles, shells, mud, coarse sands and artificial infrastructure (e.g. wind turbines). Mussel beds have an important role as ecosystem engineers since they increase habitat availability and heterogeneity (Van der Schatte et al. 2018). Despite their ecological importance, blue mussel aquaculture in Europe represents 550,000 tonnages produced per year. In the UK, shellfish aquaculture is dominated by blue mussels, which represent 95% of the production and 82% of the imputed value (Richardson 2016).

Mussel's spawning strategy is based on several mass synchronised releases of gametes from April to September, which maximises the reproductive success of the species (De Vooy 1999). The timing of spawning was previously studied using the Condition Index (CI), which calculates the ratio of shell weight to tissue weight (Filgueira et al. 2013). It has been shown that a drop in the CI corresponds to a spawning event (Duinker et al. 2008). Spawning events of *Mytilus edulis* depend on several environmental factors: air temperature, sea temperature, lunar tidal phase, geographic distribution, mussel size, age and conspecific spawning (Gardner & Skibinski 1990; Irisarri et al. 2015). Chipperfield (1953) first showed that *M. edulis* spawned initially in late May, from six distinct sites within the Irish Sea with sea temperatures rising from 10 to 13 °C. Studies in North America showed that larval spawning events for *M. edulis* occurred exclusively during spring tides (Newell et al. 1982). Younger mussels have a higher CI than older mussels, implying that it is important to investigate spawning in younger and older mussels separately (Duinker et al. 2008). Laboratory experiments have revealed that mussel spawning is induced by thermal shock, characterised by a sudden increase in seawater temperature of approximately 10 °C (Hennebicq et al. 2013; Ompi & Svane 2018).

After spawning, mussel larvae generally remain in the water column for 2–4 weeks, but can take up to 10 weeks to reach their final settlement, which is called the pelagic larvae duration (PLD) (Seed 1969). Once mussel larvae attach to a surface, they are known as spat, which will develop into adult mussels. The persistence of mussel beds depends on their self-recruitment of larvae and connectivity of larvae from surrounding mussel beds (Reaugh 2006; Commito et al. 2014). One of the largest mussel shellfisheries in the UK is in the northern part of the Irish Sea (Fig. 1B), where *M. edulis* have been successfully cultivated in the Menai Strait (North Wales) for over 50 years, due to the strong tidal currents through the Strait, which promote the flow of nutrients and water renewal (Ewins & Spencer 1967; Simpson et al. 2007). Mussel production here is based on bottom culture, which consists of harvesting wild spat that is re-laid in the area of interest for cultivation. The commercial viability of the Menai Strait depends on the collection of wild seeds from various locations in the Irish Sea and the English Channel; therefore, it is important to determine the location of wild seed beds for the Menai Strait shellfisheries (Demmer et al. 2022). Also, it is of interest to understand the impact of ‘human-made’ mussel beds on the contribution of their mussel seed to the wider environment: connectivity with the harvest beds (self-recruitment), dispersal from the Menai Strait and connectivity with natural mussel beds throughout the Irish Sea. It is assumed that mussel larvae disperse to the south of the Menai Strait, due to the persistent and strong southwest residual flow through the strait (Davies & Robins 2017). Therefore, they are thought to connect with wild mussel populations along the coasts of southwest Anglesey and the Llyn Peninsula rather than dispersing northwards through the Strait to the primary source of wild spat in the region (i.e., Liverpool Bay and Morecambe Bay).

Due to the large variability reported in the literature on mussel larvae spawning and dispersal patterns, and a lack of studies investigating larval dispersal in coastal regions, this paper addresses the following important scientific questions: (1) What are the principal factors influencing *M. edulis* gamete release? and (2) How do *M. edulis* larvae travel within well-mixed coastal environments with strong and varied tidal flows? The northern part of the Irish Sea offers an ideal opportunity to investigate these questions, being a shallow well-mixed coastal area with complex tides and coastal currents, widespread wild mussel beds and well-established shellfisheries. Field sampling over one year was undertaken to measure the Condition Index of mussels and environmental conditions to establish environmental triggers for spawning. These results were used to parameterise coupled hydrodynamic and particle tracking models to simulate larval dispersal in the coastal region – representing the first model study of larval dispersal in the Irish Sea that resolves the coastal dynamics at high resolution (e.g. at spatial scales of 20 m).

## Materials and methods

### Study area

The Menai Strait is a seawater channel located between the island of Anglesey and the mainland of North Wales. It is approximately 25 km long from Fort Belan, in the southwest, to Beaumaris in the northeast, where it re-connects with the Irish Sea. The channel has a mean width of 800 m, varying from 300 m (in the swellies area and at the southwest entrance) to 1200 m (e.g. near Caernarfon) (Kratzer et al. 2003). Water depths vary from 2 m to a maximum of 25 m in the southwest of the swellies (Campbell et al. 1998) (Fig. 1).

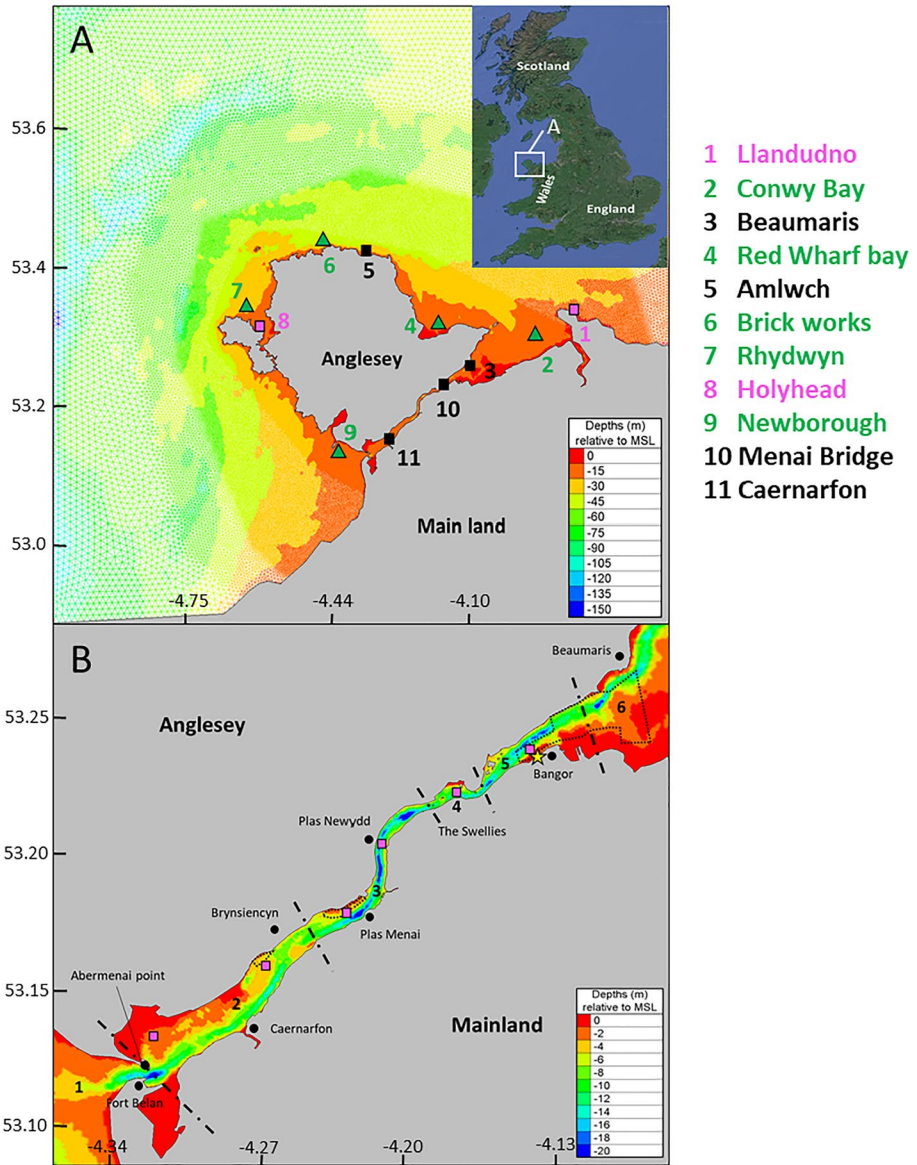


**Fig. 1** The model domain of the study region. **(A)** The hydrodynamic model with the unstructured grid resolution, the bathymetry (m), the tide gauge sites (squares) and ADCP velocity sites (triangles) used for model validation (magenta: validation by comparison of observed and simulated elevations and tidal analysis; black: sites used for tidal analysis only; and green: site used for validation only on velocity). The insert map shows the region within the UK. **(B)** Details of the Menai Strait. Bathymetry contours and key towns/ areas are shown. Mussel beds are delimited by black dotted areas. Release sites for the particle tracking modelling are represented by purple square dots. Areas used to study particle distribution are delimited by dash-dotted lines and labelled from 1 to 6. The location where sea surface temperature data were collected is represented by a yellow star

The sea bed is comprised of extensive intertidal mud flats and sandy banks; however, rocky and gravel areas are also found throughout the Strait, especially in the narrow and shallow centre (Campbell et al. 1998).

The tidal flows through the Menai Strait are strong and complex – driven by a semi-diurnal tide propagating northwards through the Irish Sea. The tidal range at the northeast entrance is greater than at the southwest entrance: 7.8 m (springs) and 2.6 m (neaps) at Beaumaris, compared with 4.8 m (springs) and 1.5 m (neaps) at Fort Belan (Campbell et al. 1998; Fig. 2a,b). These tidal differences generate an asymmetrical tidal cycle with markedly stronger currents (by 10–15%) during the ebb phase (up to 2 m/s) (Campbell et al. 1998). This means that the tidal residual flow is directed south-westwards, transporting approximately  $30 \times 10^6 \text{ m}^3$  of water over a spring-neap tidal cycle which generates a flushing time of approximately 2–3 days (Campbell et al. 1998). In the absence of wind, Davies and Robins (2017) simulated the tidally averaged volume transport to be approximately  $686 \text{ m}^3/\text{s}$  during springs and  $334 \text{ m}^3/\text{s}$  during neaps. However, Simpson (1971) reported that a strong south-westerly wind may reverse the direction of the residual flow, especially during neap conditions. Consequently, the water column is generally well mixed and vertically homogeneous in temperature (maximum difference of  $0.1 \text{ }^\circ\text{C}$  between the near surface and the near bottom) and salinity (32–34) (Rippeth et al. 2001).

### Sampling and the Condition Index calculation

*Mytilus edulis* were sampled daily from the 23rd of March 2018 to the 28th of September 2018, from the intertidal area of the commercial mussel bed located in the Menai Strait ( $53.235^\circ\text{N}$ ,  $-4.130^\circ\text{W}$ ; Fig. 1). Mussels were collected and transported to the laboratory, then scrubbed to remove all epibionts (i.e. organism living on the surface of another organism) and drained before processing.

The Condition Index (CI) was calculated based on Duinker et al. (2008). The wet weight of the total meat (in g) was recorded; also, the length (in mm) and width (in mm) of the mussel shell were measured. Based on the methods used by Slabyj et al. (1978), mussels were separated into two distinct size classes: Sample\_1:  $45 \text{ mm} < \text{shell length} < 60 \text{ mm}$

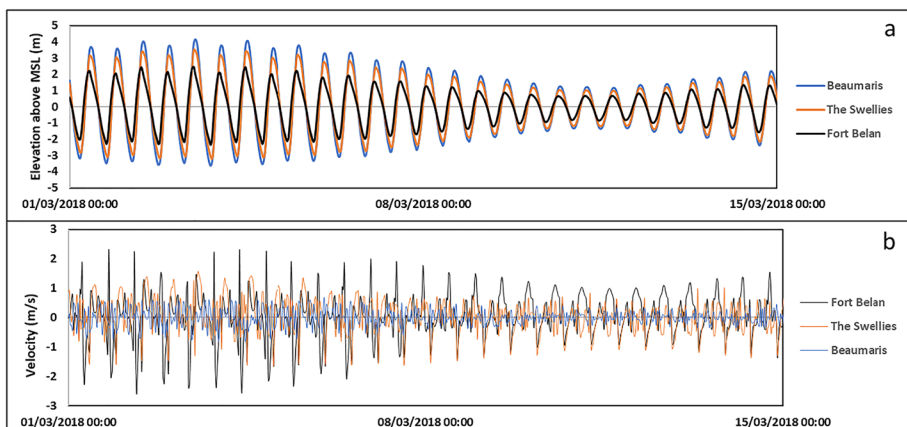


**Fig. 2** Details of the tides in the Menai Strait over a period of two weeks at three locations: Beaumaris, the Swellies and Fort Belan (see Fig. 1 for locations). (a) Time series of model simulation of the tidal range (m). (b) Time series of model simulated depth-averaged tidal flows (m/s)

and 20 mm < shell width < 26 mm; and Sample\_2: 55 mm < shell length < 65 mm and 25 mm < shell width < 30 mm. Live mussels were placed in boiling water, then the cooked meat was separated from the shells before being dried and weighed separately to calculate the Condition Index (CI) (Duinker et al. 2008):

$$CI = \frac{\text{cooked meat weight}}{\text{whole live weight} - \text{shell weight}} \times 100$$

A sudden drop in Condition Index has been proven to correspond to spawning events in previous studies, which correlate gonad observations and CI variation, for several species (fishes and bivalves mostly) and different locations (Massapina et al. 1999; Sahin et al. 2006; Li et al. 2009; Ekokotu & Olele 2014). In this study, spawning events were not measured from gonad observations; however, we assumed that a drop in the CI of 2% or more corresponds with a potential spawning as observed by Duinker et al. (2008) on *Mytilus edulis*. Environmental factors were analysed against the drop in the CI to investigate environmental spawning triggers. The environmental factors considered were (1) sea surface temperature (SST); (2) air temperature (AT); (3) wind speed and direction; (4) the phase of the lunar cycle; and (5) water elevation (WE) at the mussel bed. To study the thermal shock impact on spawning events, several scenarios were tested and the correlation coefficient was measured (i.e. measure the strength of the relationship between the relative variation of thermal difference with CI) (Table 3): (1) Does a greater daily variation of SST or AT induce a spawning event? (tests ID 1 and 2, Table 3); (2) Does a greater variation of SST or AT between the day of spawning and the day before induce a spawning event? (tests ID 3 and 4, Table 3); and (3) Does a greater difference between SST and AT on daily average value or maximum value or minimum value induce a spawning event? (tests ID 5, 6, 7 and 8, Table 3). Sea surface temperatures were recorded every 10 min with a logger located near the mussel bed (53.241°N, −4.126°W) deployed by Cefas (the logger did not record data from 26 March 2018 to 31 April 2018). Hourly wind data and AT were obtained from Valley, Anglesey (53.252°N, −4.535°W) – the nearest synoptic meteorological station – downloaded from CEDA (<https://catalogue.ceda.ac.uk>). The lunar phase was recorded daily from <https://moonphases.co.uk>. Water elevation at the mussel bed was obtained from our validated model simulation ('Hydrodynamic model').

## Hydrodynamic model

A hydrodynamic modelling approach using the Telemac system (V7p2, [www.opentelemac.org](http://www.opentelemac.org)) was applied to study *M. edulis* dispersal in the northern Irish Sea from spawning grounds in the Menai Strait. The depth-averaged Telemac-2D model is based on the shallow water approximation of the Navier–Stokes equations of momentum and continuity (Villaret et al. 2013). The finite-element numerical method is well suited to resolve complex tidal flow in coastal areas (Villaret et al. 2013). Telemac-2D is also well suited for the area of interest as the water column remains well mixed in these energetic waters throughout the year (Howarth 2005). Furthermore, high spatial resolution (~20 m) can be achieved with Telemac's unstructured mesh configuration to sufficiently resolve coastal areas for larval transport, where structured 3D models would be computationally expensive and impractical over large domains and long periods required for simulating dispersal.

The mesh density, created with Blue Kenue™ grid generation software, varies from 1000 m on the outer boundary in the Irish Sea to 100 m along the coast of Anglesey (Fig. 1A). Within the Menai Strait and adjacent coastline, the mesh density varies from

50 m at the approaches to the strait to 20 m in the interior to resolve accurately the complex tidal currents around features such as islands and bridge piers (Fig. 1A). The unstructured grid comprises 187,295 nodes over an area of 10,000 km<sup>2</sup>. The grid was mapped onto bathymetric data comprising an assemblage of (1) multi-beam data collected during 2012 (high resolution: ~5 m); (2) LiDAR data collected during 2013 (high resolution: ~2 m); and (3) Admiralty bathymetric data of the offshore regions at both ends of the Strait (interpolated onto a 200 m horizontal resolution grid) (Davies & Robins 2017). Constant coefficient friction of 0.1 was implemented in Nikuradse's law of bottom friction. Five tidal constituents forced the model at the open boundary using the TPX07-v2 database: semi-diurnal lunar ( $M_2$ ) and solar ( $S_2$ ), together with larger lunar elliptic ( $N_2$ ), luni-solar diurnal ( $K_1$ ) and principal lunar diurnal ( $O_1$ ). The model was initially spun-up for one month (February 2018). The model was then run for one month (March 2018), and the model outputs (e.g. depth-averaged velocity and water elevation) were stored every 30 min for subsequent processing as it was sufficient to resolve the flow fields (sensitivity tests data not shown).

## Model validation

Surface elevations and depth-averaged velocities from the March 2018 simulation were compared against time series of sea levels from tide gauges (data from the British Oceanographic Data Centre, BODC) and velocities from offshore moorings (data from Bangor University). For the water elevation comparison, two tide gauge sites were used within the study area: Holyhead and Llandudno. For the velocity comparison, five sites were used to compare magnitude (Fig. 1). Validation was achieved using the root mean square error (RMSE) and the normalised root mean square error (NRMSE in %) between the observations and model outputs:

$$RMSE = \sqrt{\frac{\sum_{i=1}^n (y_i - \hat{y}_i)^2}{n}}$$

$$NRMSE = \frac{RMSE}{\hat{y}_{\max} - \hat{y}_{\min}}$$

where  $y_i$  and  $\hat{y}_i$  represent respectively the  $i$ th value of observed and simulated data (for water depth in m and for velocity magnitude in m/s);  $\hat{y}_{\max}$  and  $\hat{y}_{\min}$  correspond to the maximum and minimum value of the simulated data.

In addition, tidal analysis was performed using the T-tide Matlab toolbox, in order to compare the primary semi-diurnal lunar tidal constituent ( $M_2$ ) between the simulated and observed data (taken from Admiralty tidal stream atlas).

## Particle tracking model simulations

A Lagrangian particle tracking model (PTM) was developed to predict the likely dispersal of *M. edulis* larvae from known mussel beds in the northern Irish Sea. Simulated depth-averaged velocities output from the hydrodynamic model were linearly interpolated from 30 to 5 min (computational limit) and used to drive the PTM. Six particle release sites were chosen: (1) where there are commercial mussel beds present (Bangor); (2–3) non-commercial mussel beds (Plas Menai and Brynsiencyn); and

in regions of geographic interest: (4) the Swellies because of the strong and complex currents; (5) Plas Newydd because of its location at mid-channel; and (6) Abermenai Point because since the location controls the southwest exit of the Strait (Fig. 1). Cohorts of 7000 larvae were released from each site scattered randomly within an area of 0.1 km<sup>2</sup> (previously determined by sensitivity test on the size of the released patch; Demmer 2020). These values were developed through a model sensitivity test to create the most efficient PTM in time whilst simulating sufficient particles to adequately capture the dispersal.

Particles were dispersed by advection and sub-grid-scale diffusion according to Proctor et al. (1994) and Ross and Sharples (2004):

$$x(it + 1, ip) = x(it, ip) + U * \Delta t + x_{\text{diffusivity}}$$

$$y(it + 1, ip) = y(it, ip) + V * \Delta t + y_{\text{diffusivity}}$$

with

$$x_{\text{diffusivity}} = \frac{A}{r} * \cos(2\pi A) * \sqrt{2K\Delta t}$$

$$y_{\text{diffusivity}} = \frac{A}{r} * \sin(2\pi A) * \sqrt{2K\Delta t}$$

where  $x$  and  $y$  are the coordinates along the absciss and ordinate (m), respectively;  $U$  and  $V$  are the corresponding velocities (m/s);  $\Delta t$  is the PTM timestep (s);  $A$  is a random number in the range  $[-1, 1]$ ;  $r$  is the standard deviation of  $A \cos(2\pi A)$  with a value of  $1/\sqrt{6}$ ; and  $K$  is the coefficient diffusion with a value of 5 (m<sup>2</sup>/s). Particle positions were spatially bilinearly interpolated for each iteration of the PTM (i.e. every 5 min) to accurately capture the evolving velocity field.

Due to the strong tidal currents in the region (up to 3 m/s), no active larval transport was parameterised in the model as any vertical migration behaviour of the larvae would have minimal impact on their horizontal dispersal (Pernet et al. 2003). Also, no mortality was implemented as this would reduce the data size for the statistical analysis, and because there is insufficient information on mortality rates during the larval phase (Horvath & Crane 2010). Furthermore, if particles were advected onto land, they were reflected back to their position in the previous model time step (North et al. 2008; Coscia et al. 2013). The particle tracking model does not take into account the bathymetry gradient as it is small compared to the velocities (Pearson & Barber, 1998). This study focuses on the first week of PLD to qualify and quantify the transport of particles away from the coastal spawning bed, e.g. dispersal within/through the Menai Strait and along the coastline of North Wales. In reality, the PLD of *M. edulis* varied from 2 to 4 weeks, but it can take up to 10 weeks to reach the final settlement (Seed 1969). Each particle position was recorded every 30 min until the end of the simulation (one week).

Eight simulations were performed, with the release time shifted according to the tide. Four simulations started during spring tides when water elevation was (1) high water (HW); (2) low water (LW); (3) mid-water-ebb; and (4) mid-water-flood (Fig. 3). The same four scenarios were applied during neap tides. At the end of each simulation,



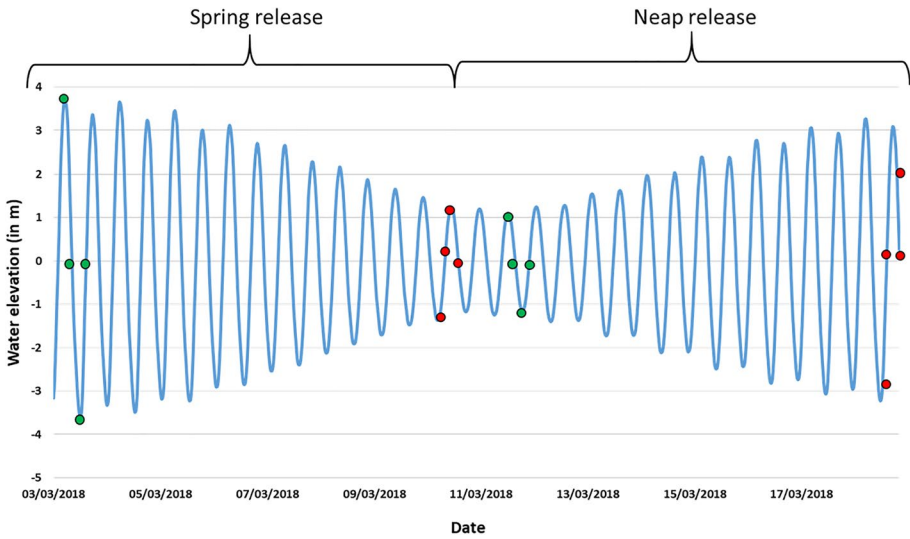


**Fig. 3** Simulated time series of water elevation at Bangor showing the release time of particles (red dots) and end of the simulation (green dots)

a total of 56,000 particles were present in the domain which represented 336,000 particles across all simulations (i.e. 6 release sites × 7000 particles × 8 release dates).

**Analysis methods**

The coast surrounding the release sites was divided into six areas, as presented in Fig. 1, to estimate the proportion of larvae within each area after one week depending on (1) the location of release and (2) the timing of release with respect to the tidal cycle. The effect of the tidal phase on particle dispersal was represented in three ways: (1) comparison of neap vs spring tides (four simulations per tide); (2) comparison of ebb vs flood tides releases (two simulations per tide); and (3) comparison of HW vs LW releases (two simulations per tide). All results are presented as density distribution maps, and differences between simulated distributions > 60% were assumed to be significant. Finally, the tidal averaged currents and the difference of tidal averaged currents (over one week) were calculated between simulations starting during spring tide and simulations starting during neap tide to understand the difference of distribution for the different tidal scenarios tested.

**Results**

**Validation**

Results showed NRMSE for water elevation was 4.8% which corresponds to 35 cm, on average for the two sites, with a higher difference during spring tide (approx. 50 cm) than during neap tide (approx. 25 cm) (Fig. 4 and Table 1). Velocity magnitude showed

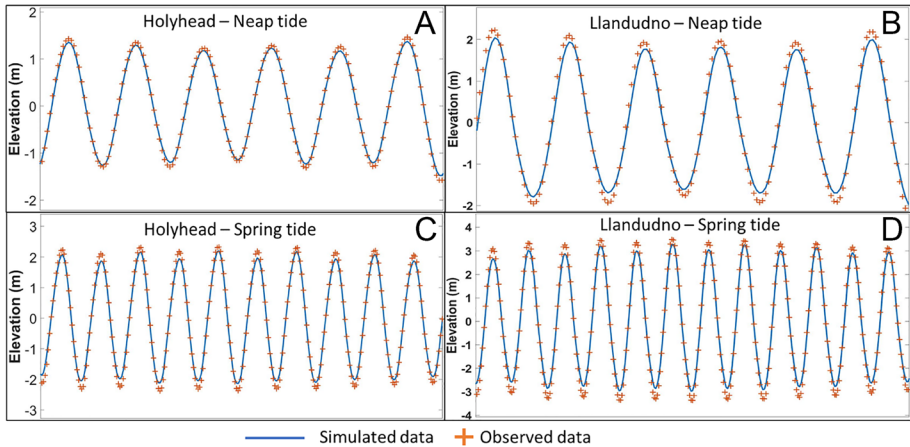


**Fig. 4** Time series of surface elevation (m) in March 2015 during (1) neap tide at Holyhead (A) and Llandudno (B) and (2) spring tide at Holyhead (C) and Llandudno (D). Simulated data (blue solid line) and observed data (cross) are represented

NRMSE results of 13.6% lower, on average, for five sites (Fig. 5 and Table 1). Results showed that NRMSE varied according to the site and the tidal cycle. We noticed a better NRMSE at Conwy Bay during neap ( $-0.025$  m/s) tide than spring tide ( $-0.05$  m/s) (Fig. 5A,C), whereas at Rhydwyn, NRMSE is smaller during spring than neap (Fig. 5B,D). Tidal analysis showed a difference of 1% between simulated and observed data on average for six sites (Table 1).

### Larval spawning times

The set of mussels with a smaller size (Sample\_1), collected from the Bangor mussel bed during spring and summer of 2018, had a mean shell length of 50.9 mm and shell width of 23.1 mm, while the set with a bigger size (Sample\_2) had a mean shell length of 59.9 mm and width of 26.6 mm (Fig. 6). The observed difference between the sampled means was significant for both width and length, meaning that these two groups can be analysed independently.

The variation of the CI over the period of the study showed a correlation of 0.94 between Sample\_1 and Sample\_2. Indeed, Fig. 6 shows that the CI followed three clear trends for both samples: (1) a decrease in the CI from the end of March to the start of May to reach minimum values of 17.28% (Sample\_1) and 16.40% (Sample\_2) ( $R^2=0.37$ ); (2) an increase in the CI from the start of May to the start of July with maximum values of 32.31% (Sample\_1) and 27.33% (Sample\_2) ( $R^2=0.85$ ); and (3) a decrease in the CI from July to the end of September ( $R^2=0.35$ ). Furthermore, the mean CI of Sample\_1 was 9.30% higher than Sample\_2 over the period of study (Fig. 7). The CI variation through spring/summer positively correlated to the variation of SST ( $R^2=0.80$ ) (Fig. 7). The maximum temperature occurred during July with values of 18.57 °C (SST).

During the survey, the three largest drops in the CI for both sample sets occurred: (1) 26–27 March (decreased by 4.21% for Sample\_1 and 5.55% for Sample\_2); (2) 22–23 April (decreased by 3.28% for Sample\_1 and 3.73% for Sample\_2); (3) 20–21 September (decrease by 4.07% for Sample\_1 and 3.40% for Sample\_2) (Fig. 8 and Table 2). The three

**Table 1** Model validation for (1) surface elevation (during March 2018) showing RMSE (m) and NRMSE (%); (2) simulated velocity magnitude (m/s) and NRMSE (%); and (3) tidal analysis of the M2 tidal constituent (%) (The mean values are represented in bold)

Sites	1	2	3	4	5	6	7	8	9	10	11	Mean
Elevation	RMSE (m)	0.35	-	-	-	-	-	0.34	-	-	-	<b>0.35</b>
	NRMSE (%)	5.5	-	-	-	-	-	4.04	-	-	-	<b>4.77</b>
Velocity magnitude	RMSE (m/s)	-	0.08	-	0.07	0.21	0.16	-	0.07	-	-	<b>0.12</b>
	NRMSE (%)	-	14.58	-	13.28	10.65	13.19	-	16.52	-	-	<b>13.64</b>
Tidal analysis	Difference (%)	-1.3	-	-2.9	-	0.8	-	-1.2	-	-0.3	-1.1	<b>-1</b>

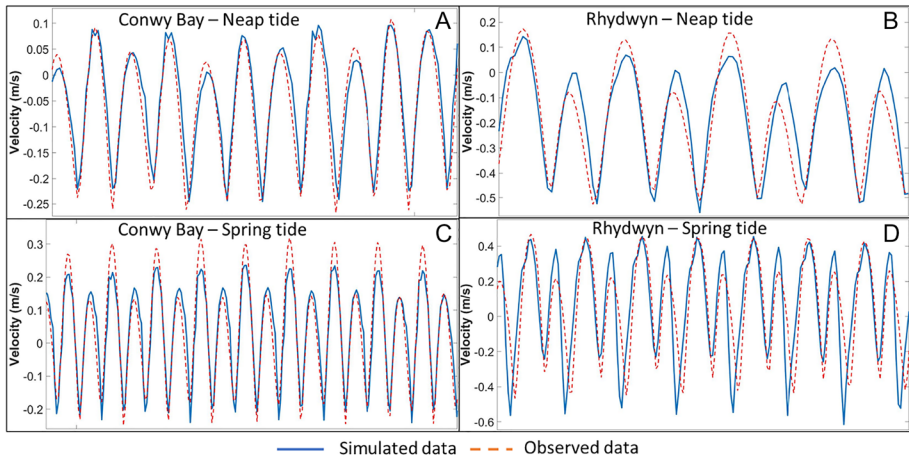


**Fig. 5** Time series of velocity (m/s) in November 2015 during (1) neap tide at Conwy Bay (A) and Rhydwyn (B) and (2) spring tide at Conwy Bay (C) and Rhydwyn (D). Simulated data (solid blue line) and observed data (dotted line) are represented

largest drops in the CI happened one or two days after an increase in SST (by  $2.4\text{ }^{\circ}\text{C} \pm 0.2\text{ }^{\circ}\text{C}$ ) and AT (by  $2.18\text{ }^{\circ}\text{C} \pm 0.47\text{ }^{\circ}\text{C}$ ) and when AT was lower than SST by  $3\text{ }^{\circ}\text{C}$ , on the mean (Fig. 8; drops shown by black arrows).

Small drops of the CI were observed several times for each sample group, with ten of these events occurring: (A) for Sample\_1: 5 April, 13 April, 1 May, 28 June, 11 July, 24 August and 6 September; (B) for Sample\_2: 31 March, 24 May, 12 June and 11 July (Fig. 8; drops shown by grey arrows). In most cases, these fluctuations happened when the difference between AT and SST was greater than  $1\text{ }^{\circ}\text{C}$ , except for 12 June and 11 July, where the AT dropped by  $1.62\text{ }^{\circ}\text{C}$  and  $2\text{ }^{\circ}\text{C}$ . Results also showed that for all small CI fluctuations events, SST increased by  $0.52\text{ }^{\circ}\text{C}$  on the mean.

However, no significant correlation was observed between the thermal difference conditions tested and the variation of CI. Indeed, results showed that the correlation coefficient ( $R^2$ ) is very low for all scenarios tested (Table 3).

The three biggest drops of the CI occurred when the lunar phase was in its third quarter (i.e. few days before neap tides, when the water elevation did not exceed 2.5 m above the mussel bed), whilst the smaller drops of the CI occurred when the lunar phase was close to the full moon or new moon (Fig. 9). No correlation was observed when the drop of the CI was compared with the wind data (strength and direction) (Fig. 9).

## Larval dispersal

Results showed that 48% of the particles dispersed out of the Menai Strait within one week, on average for all simulations (e.g. release sites and tidal scenarios). As we expected, many of the particles (45%) exited from the south of the Strait (into area 1), due to the strong and persistent southwest tidal averaged current, on average for all sites and simulations. However, 3% of the particles dispersed north from the Strait into area 6, on average for all sites and simulations. The remaining 52% of the particles were retained within the Menai Strait within one week (39% in the Swellies (area 3), 7% in Plas Newydd (area 4), 5% in Caer-narfon (area 2) and 1% in Bangor (area 5)), on average for all sites and simulations.

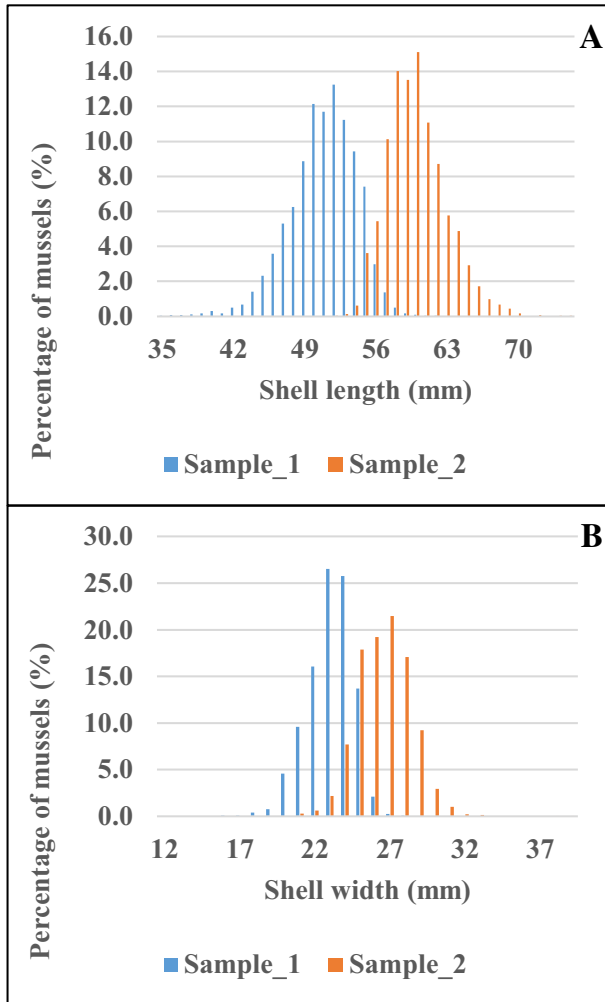


**Fig. 6** Mussel distribution among Sample\_1 (in blue) and Sample\_2 (in orange) depending on (A) shell length and (B) shell width

Different larval dispersal patterns were observed depending on the six discrete release sites within the Strait, although a common result was that the mid-channel narrowing (at the Swellies) acted as a trapping region (sink) for larvae dispersing northwards and southwards (73% of particles trapped) (Fig. 10). For particles released from the Bangor mussel bed, 8% exited towards the south while 12% exited towards the north (Figs. 10A and 11). For particles released from Abermenai Point, 94% exited from the south and no particles dispersed further north than the Swellies (Figs. 10F and 11). Similar results were simulated for particles released from Brynisiencyn (72% exited the south) and <0.5% dispersed north of the Swellies (Figs. 10E and 11). For particles released from the Swellies, 68% remained in the same area within one week (Figs. 10B and 11). Similarly, 40% of the particles released from Plas Newydd and Plas Menai were trapped in the Swellies, while 2% exited from the north and 40% from the

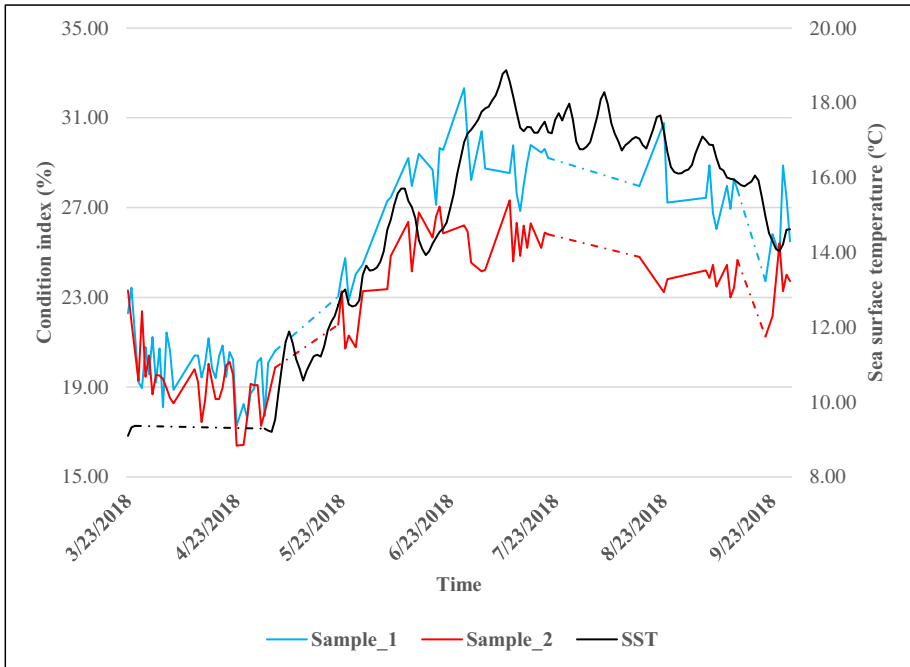


**Fig. 7** Evolution of (1) Condition Index for Sample\_1 (in blue) and Sample\_2 (in red) over spring/summer 2018 and (2) sea surface temperature (SST) in black. The proportion of the curves in dashed line corresponds to the period when data were not collected

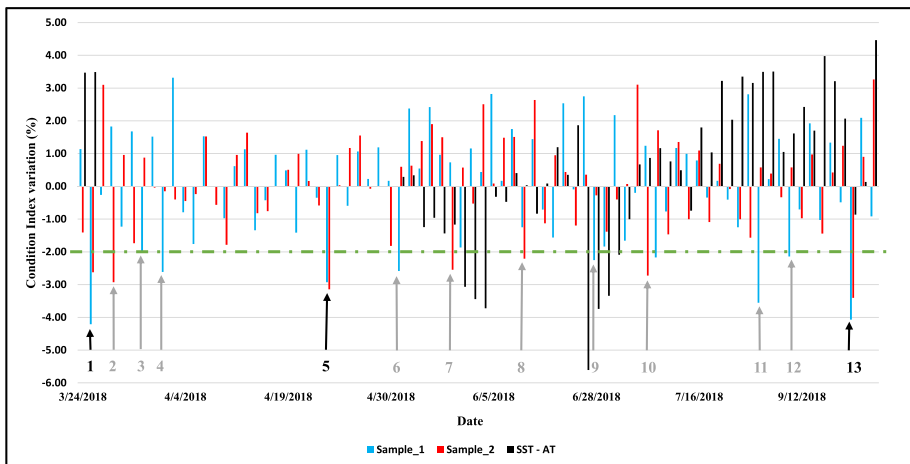


**Fig. 8** Variation of (1) Condition Index for Sample\_1 (in blue) and Sample\_2 (in red) over spring/summer 2018 and (2) difference between sea surface temperature (SST) and air temperature (AT) in black. The green, dashed and dotted line corresponds to the threshold drop in CI corresponding to a spawning event. Black arrows point to days of assumed massive spawning events (drop of CI > 2% and simultaneous for the two samples), and grey arrows point to days of assumed small spawning events (drop of CI > 2% but not simultaneous for the two samples)

**Table 2** Biggest drop of CI with the corresponding (1) date, (2) CI variation in % for both samples, (3) SST difference between the day of spawning and the day before, (4) AT difference between the day of spawning and the day before and (5) difference between AT and SST in °C

Spawning events	Date	CI variation (%)		SST variation (°C)	AT variation (°C)	AT–SST (°C)
		Sample 1	Sample 2			
1	26/27 March	–4.21	–5.55	0.26	2.00	–3.49
2	22/23 April	–3.28	–3.73	N/A	2.75	N/A
3	20/21 September	–4.07	–3.40	0.22	1.80	–2.56

**Table 3** Correlation between thermal difference tested against Condition Index variation with (1) sea surface temperature (SST), (2) air temperature (AT) and (3) spawning day (SD)

Test ID	Thermal shock tested	Correlation coefficient	
		Sample 1	Sample 2
1	$SST_{(max)} - SST_{(min)}$	3.10–2	1.10–2
2	$AT_{(max)} - AT_{(min)}$	2.10–2	2.10–2
3	$SST_{(max, day-1)} - SST_{(min, day)}$	3.10–4	2.10–3
4	$AT_{(max, day-1)} - AT_{(min, day)}$	5.10–5	8.10–4
5	$SST_{(average)} - AT_{(average)}$	1.10–2	4.10–5
6	$SST_{(max)} - AT_{(max)}$	9.10–3	2.10–2
7	$SST_{(min)} - AT_{(min)}$	3.10–3	4.10–3
8	$SST_{(min)} - AT_{(max)}$	2.10–2	1.10–2

south (Figs. 10C,D and 11). For all the particles that exited from the north of the Strait after one week, approximately 55% were released from Bangor and 25% from the Swellies (Fig. 10). On the other hand, release sites south of the Swellies (Abermenai Point, Brynsiencyn, Plas Menai and Plas Newydd) contributed to 90% of particles that exited the south of the Strait (Figs. 10 and 11). Releasing particles from Plas Newydd showed an equal distribution within areas 2, 3, 4 and 5 (~20% for each) and ~11% for areas 1 and 6 (Figs. 10C and 11).

The simulations showed different particle dispersal patterns between the tidal phase within one week, although a clear correlation between the tidal phase and dispersal was not detected. Most of the particles that exited from the south of the Strait were released during neap ebb (74.6%), neap LW (52.7%), spring ebb (43.4%) and spring HW (59.1%) (Table 4 and Fig. 12A,D,E,G). When particles were released during neap flood (51.4%), neap HW (47%), spring flood (46.8%) and spring LW (52.5%), a majority of them were trapped in the Swellies (area 3) (Table 4 and Fig. 12B,C,F,H). For all release tidal periods simulated, the distribution was minimal near Bangor (area 5) (Table 4 and Fig. 12). Also, particles released during neap flood (5.7%), spring ebb (5.18%) and spring LW (6.4%) exited the Menai Strait from the north (area 6) (Table 4 and Fig. 12B,E,H).

The comparison between neap and spring tides showed no difference among areas except for Bangor (area 5) (Fig. 13A). Indeed, the spring tide release contributed to 81% of the particles found in the Bangor area after one week. Furthermore, Fig. 12 shows that when particles were released during neap tide, they were found further south, along the Llyn peninsula (area 1). Equal proportions of particles released during ebb or flood

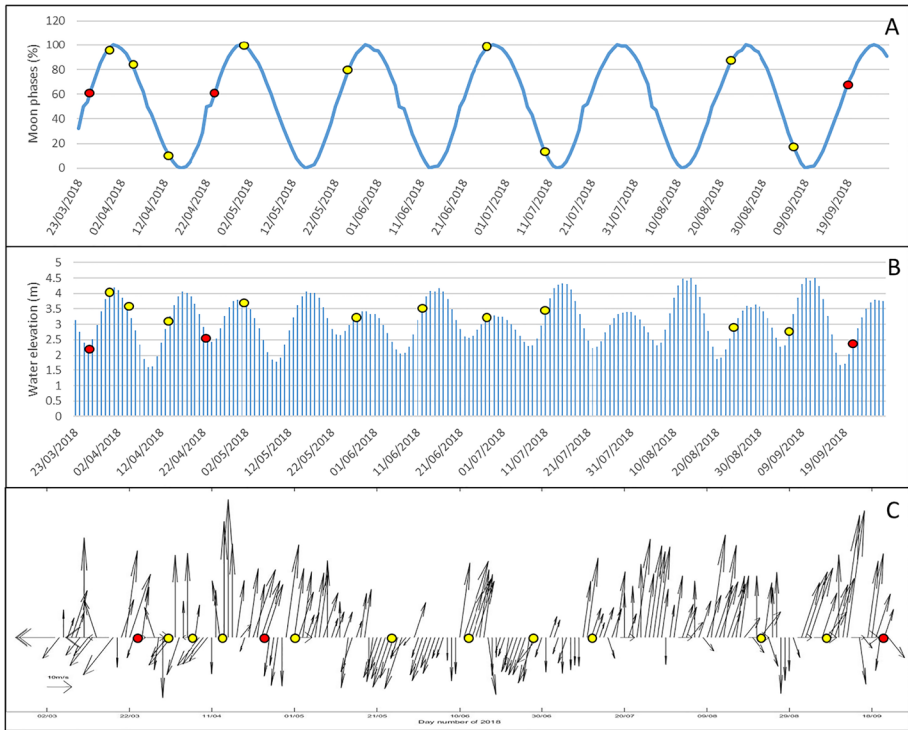


**Fig. 9** Evolution of (A) lunar phase in % with full moon represented by 100% and new moon represented by 0%, (B) water elevation in m and (C) wind strength and direction by arrows. Red dots represent the assumed massive spawning events, and yellow dots represent the assumed small spawning events

tides dispersed to Plas Newydd and Bangor (areas 3 and 5) (Fig. 13B). However, particles released during ebb tide were more likely to exit from the south of the Strait (65%) than particles released during a flood (Fig. 13B). Particles released during HW or LW showed no significant difference in dispersal patterns (Fig. 13C). Particles released at LW contributed mostly ( $65\% \pm 5\%$ ) to the particles found in areas 3, 5 and 6 (Fig. 13C).

## Discussion

### Larval spawning time

Blue mussel larval spawning events have been inferred from sharp drops in their Condition Index (CI) (Duinker et al. 2008). By applying this assumption for this study, observations of CI from Irish Sea (Menai Strait) mussels indicated that there were multiple spawning events throughout the spring and summer of 2018. The first major event occurred at the end of March, which is considered relatively early, when sea surface temperatures were about  $9\text{ }^{\circ}\text{C}$  but with a sharp rise in air temperature reaching  $25\text{ }^{\circ}\text{C}$  for 2 days – potentially inducing this earlier spawning. Subsequent major spawning events occurred in late April



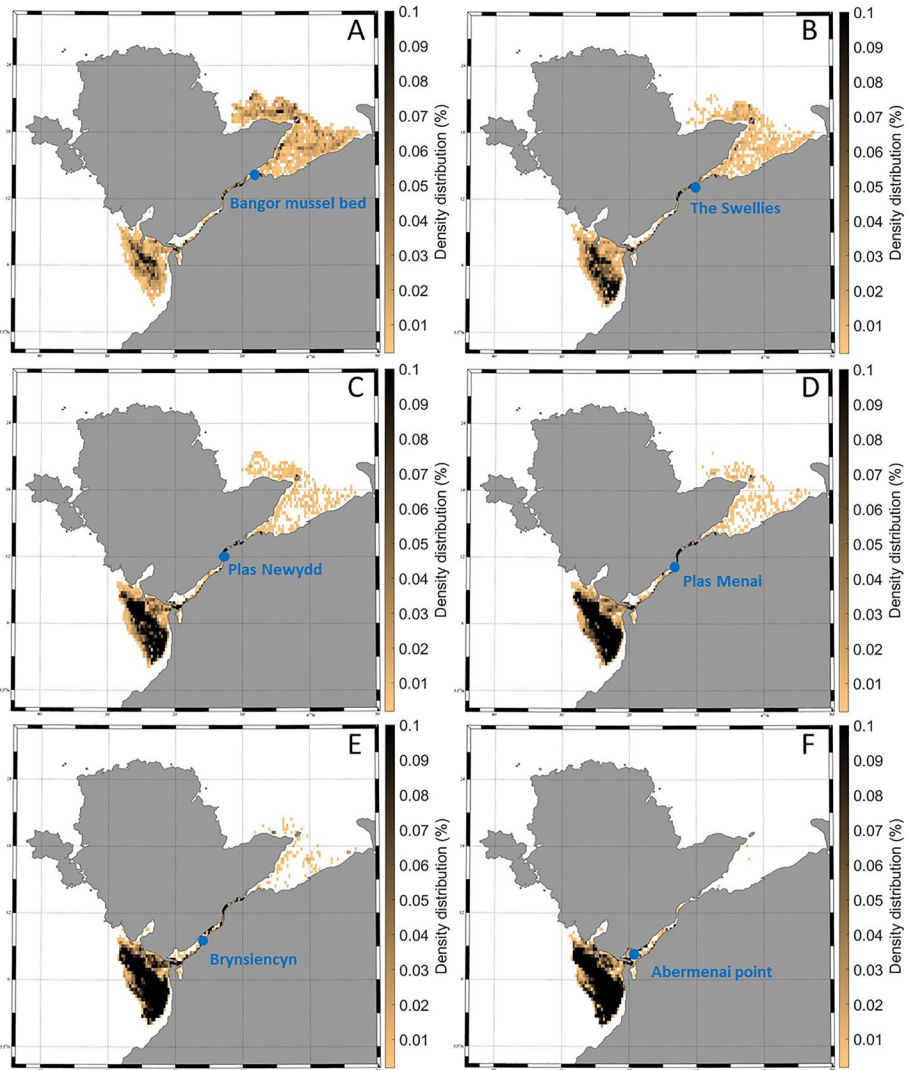


**Fig. 10** Density distribution of mussel larvae after one week with released area represented by a blue dot: (A) Bangor mussel bed, (B) the Swellies, (C) Plas Newydd, (D) Plas Menai, (E) Brynslencyn and (F) Abermenai point

and late September, which coincide with the spawning period observed previously (Chipperfield 1953; Duinker et al. 2008).

In nature, mussels in the intertidal area can be subjected to a thermal shock if the difference between air temperature (AT) and sea surface temperature (SST) exceeds a particular threshold. The observations here revealed here several occasions when the SST was ~2.5 °C higher than the AT. However, no strong correlation was made in this study between the major drops in CI and a range of observed AT/

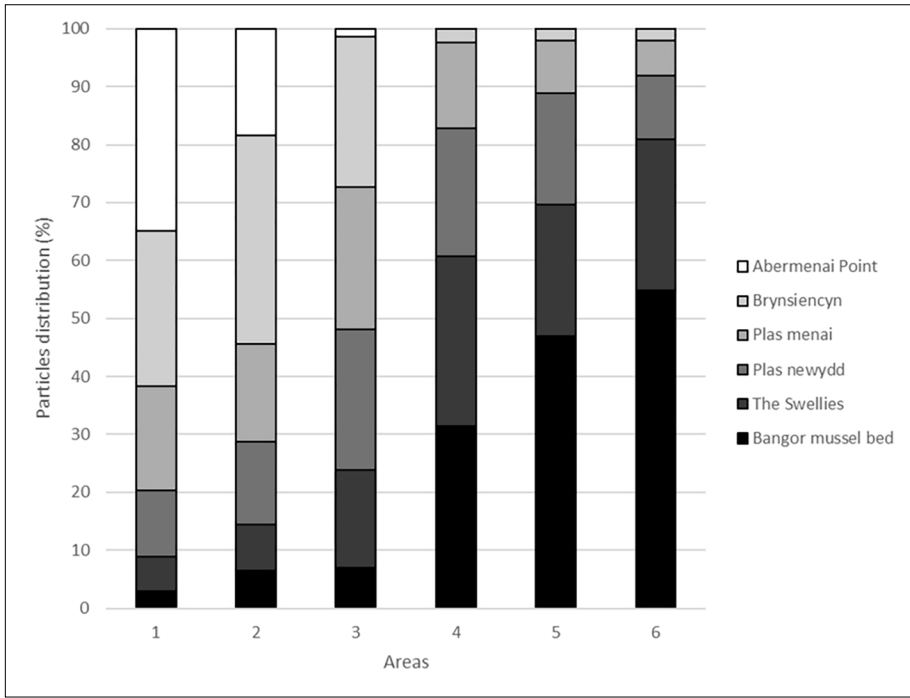


**Fig. 11** Particles distribution in % for 6 areas of interest depending on the release site. The areas of interest are (1) south of the Menai Strait, (2) Caernarfon, (3) Plas Newydd, (4) the Swellies, (5) Bangor and (6) north of the Menai Strait. The sites of released are represented in (1) black for Bangor mussel bed, (2) light black for the Swellies, (3) dark grey for Plas Newydd, (4) medium grey for Plas Menai, (5) light grey for Brynsiencyn and (6) white for Abermenai point

**Table 4** Particles distribution in % for the 6 areas depending on the release tidal period

Release tide	Areas					
	1	2	3	4	5	6
Neap ebb	74.61	3.29	3.49	17.91	0.15	0.55
Neap flood	31.83	3.04	7.61	51.41	0.38	5.73
Neap HW	36	7.38	5.78	47.04	0.38	3.42
Neap LW	52.67	3.54	10.71	29.89	0.24	2.95
Spring ebb	43.4	4.1	13.11	32.43	1.78	5.18
Spring flood	32.37	8.28	7.19	46.79	1.6	3.77
Spring HW	59.1	4.92	3.28	31.41	0.52	0.77
Spring LW	27.55	5.92	6.48	52.52	1.13	6.4
Mean	44.69	5.06	7.21	38.68	0.77	3.6

*The areas of interest are (1) south of the Menai Strait, (2) Caernarfon, (3) Plas Newydd, (4) the Swellies, (5) Bangor and (6) north of the Menai Strait. The highest values are represented in orange; the lowest values are represented in blue; the mean values are represented in red*

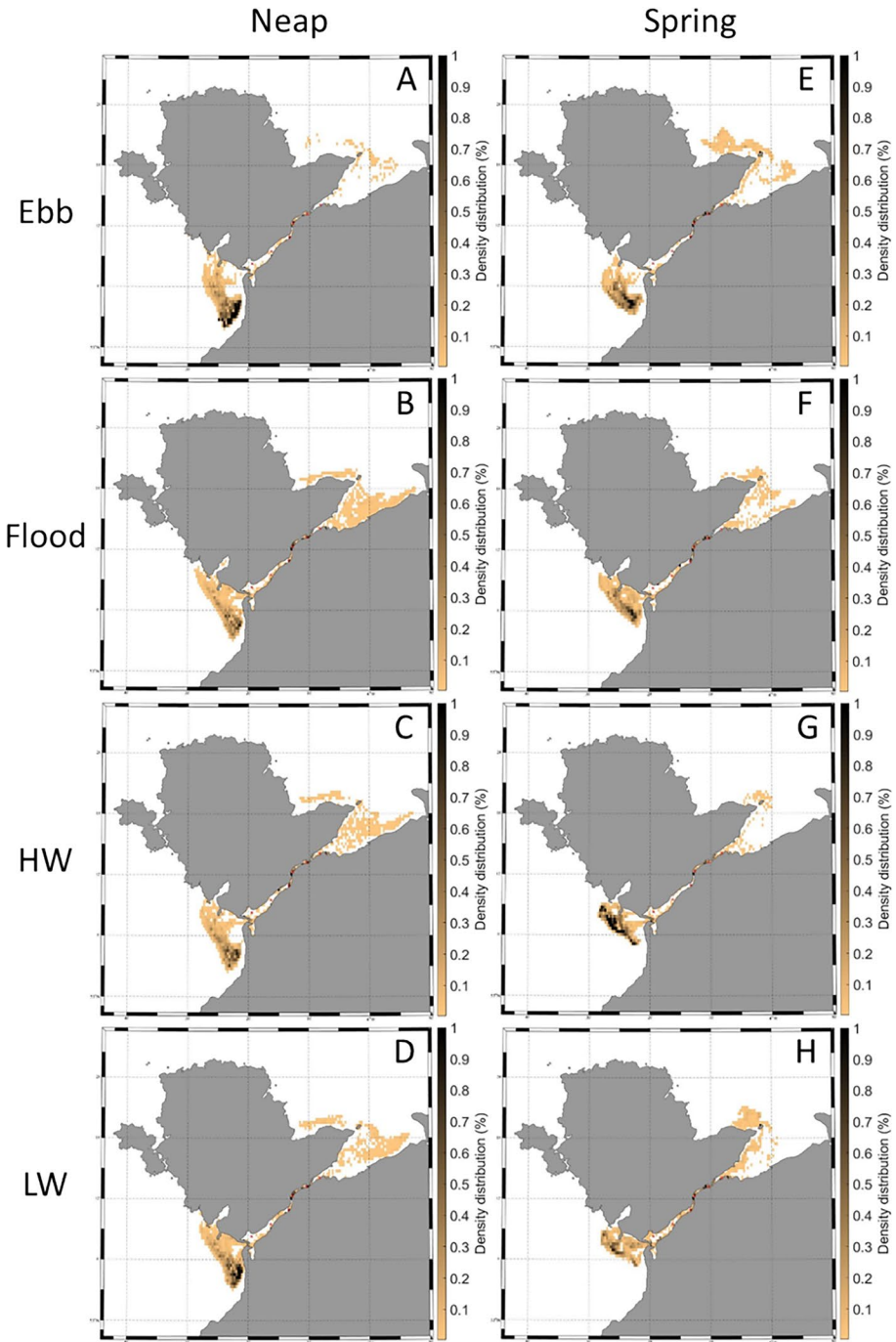


**Fig. 12** Density distribution of mussel larvae after one week depending on the tidal phase during particle release (A) neap ebb, (B) neap flood, (C) neap HW, (D) neap LW, (E) spring ebb, (F) spring flood, (G) spring HW and (H) spring LW

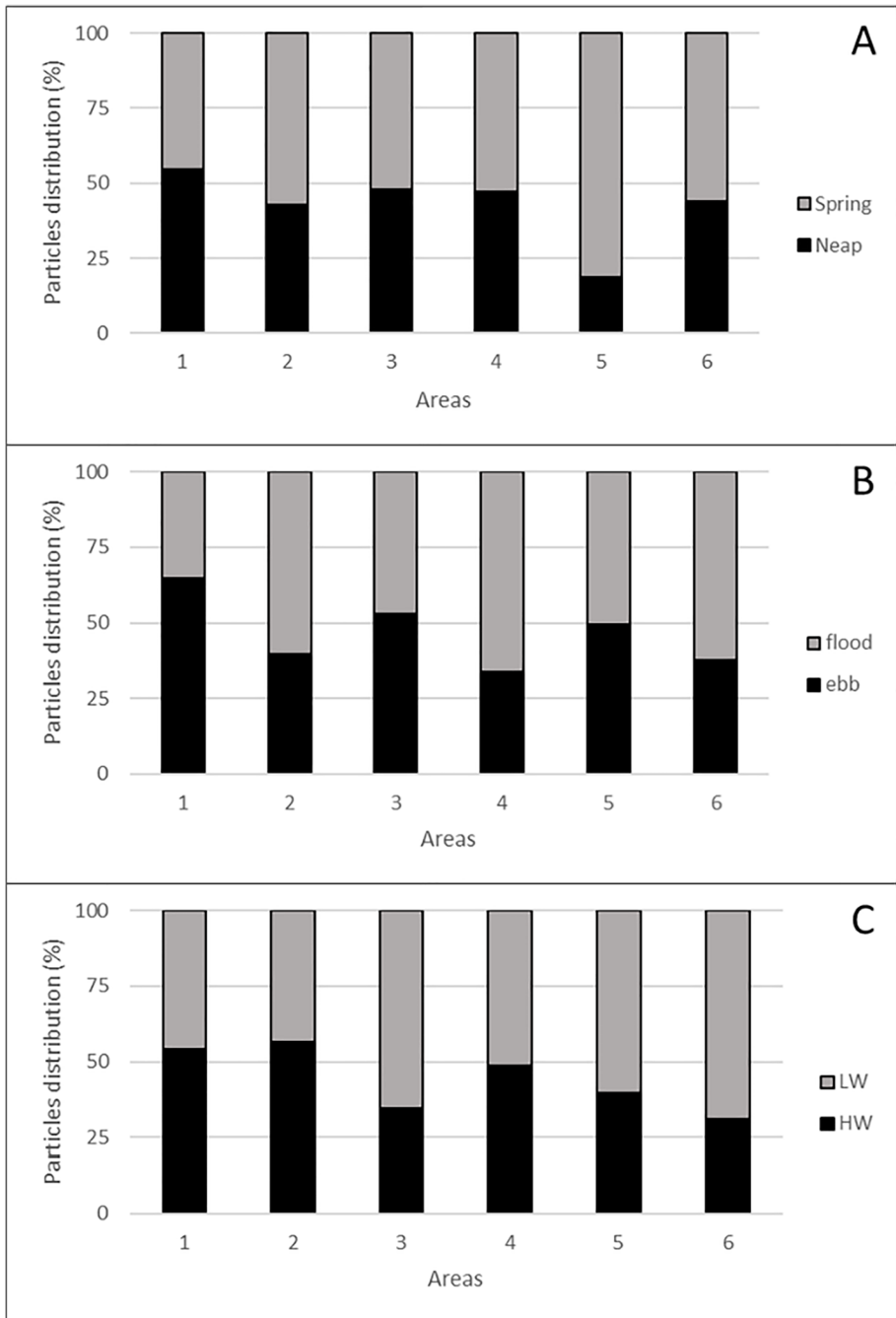


**Fig. 13** Particle distribution in % for 6 areas of interest depending on the release tide. The areas of interest are (1) south of the Menai Strait, (2) Caernarfon, (3) Plas Newydd, (4) the Swellies, (5) Bangor and (6) north of the Menai Strait. Particles were released at (A) spring tide in grey and neap tide in black, (B) flood tide in grey and ebb tide in black and (C) LW in grey and HW in black

SST thermal ‘shock’ thresholds, which is contrary to other studies (Duinker et al. 2008). Larval spawning has previously been described by Doherty et al. (2009) on a monthly scale which showed a massive drop between March to May. However, no information is given on the possibility of several spawning events. Here, the study analyses the CI on daily observations showing that the monthly drop of CI is the consequence of consecutive spawning of different intensities with trickle spawning events in between larger events.

The Condition Index of the samples showed the same three clear trends which we suggest can be explained as follows: (1) During March to May, the reduction in the CI was assumed to be the consequence of two main spawning events on 26 March and 22 April. (2) An increase in the CI from May to July can be explained by the presence of a phytoplankton bloom, which would increase the availability of food as *M. edulis* feed on phytoplankton to build their own biomass (Gowen et al. 1995; Gowen & Stewart 2005; Fernandez et al. 2015). (3) A decrease in CI from the end of July to September is due to the decrease in food availability and successive spawning events (Gowen & Stewart 2005).

As mussels were collected from a single intertidal mussel bed, the impact of environmental parameters (e.g. air temperature, lunar phase, sea surface temperature, food availability and geographic distribution), which influence the mussel growth rate (Bergstrom & Lindegarh 2016) were the same for the small (Sample\_1) and large (Sample\_2) mussel groups analysed. Therefore, the relative mean size of each sample gave an indication of their relative ages, with mussels from Sample\_1 being considered younger (because they were smaller) than those from Sample\_2. The results showed that the sample-averaged CI was consistently higher for the younger mussel by almost 10%. Similar observations were made previously for *M. edulis* (Slabyj et al. 1978; Dare & Edwards 1975 and Sprung 1984). However, the difference between the samples in the Menai Strait was greater (almost 10%) than observed in Norway (5%) by Duinker et al. (2008). The difference in temperature of the water between Norway and North Wales and its impacts on food availability for *M. edulis* could explain this result (Smaal & van Stralen 1990).

In the Menai Strait, the results showed that the main CI drop (spawning) events occurred during the third-quarter lunar phase, approaching neap tides, contrary to the result from Newell et al. (1982), who observed spawning during spring tides in North America. In North Wales, spring low water always occurs approximately during mid-morning (06:00) and late-afternoon (18:00), whereas neap low water occurs during midday and midnight. During neap tides, therefore, intertidal mussels are exposed to minimal (midnight) and maximal (midday) air temperatures each day. Yet, as stated above, no strong correlation was made between CI and daily thermal difference. Further investigations should be conducted on the hydrostatic pressure, which might cause stress on the feeding rate, for example, and so influence spawning (Battle 1931; Famme et al. 1986). Holt and Proctor (2003) showed that wind influences AT and SST in the Irish Sea; however, we found no strong correlation between the wind direction and strength of CI drops. Hence, our study suggests that spawning events of mussels in the Irish Sea are the results of more complex interactions between the organisms and their environment than solely a thermal shock, as seen in laboratory experiments. Further studies should work on the impact of food availability on mussel spawning events as it has been previously shown that the quality and abundance of phytoplankton can influence spawning patterns (Ram et al. 1996).

## Larval dispersal

Considering all the PTM simulations performed, 95% of the particles released within the Menai Strait either remained within the channel or travelled south during their initial week, with only 5% remaining in the northern part of the Strait. These results are consistent with the literature, which confirmed a persistent southwest residual current through the Strait (Simpson et al. 2007; Davies & Robins 2017). For the particles that remained within the Menai Strait after one week (52%), the majority of them (39%) were trapped in the narrow/shallow mid-section known as the Swellies. Furthermore, 68% of particles released from the Swellies remained there. These results are different from those presented by Harvey (1968), whereby drifters located in the Swellies after one week represented 1.7% of all the drifters released. However, the comparison was not exactly as the drifters were released from different locations and during different dates. Nevertheless, the PTM may over-predict particle retention within this narrow (width of 250 m) part of the channel. Indeed, Demmer et al. (2022) showed that particles, simulated over a longer period and including other parameters (such as wind), do not get trapped in the Swellies. Although the model was configured to maximise the spatial and temporal resolution of the flow field through the Swellies (PTM timestep of 5 min and 20 m mesh) whilst being computationally practical.

It has been shown that larvae can travel within an area < 100 km along the coast of South Africa and can be found up to 10 km offshore within a week due to the Agulhas current (Weidberg et al. 2015). However, here, we show that larval transport along a topographically complex/undulating coast can drastically reduce their dispersal potential. For example, larvae tended to travel < 15 km in our study, even though the tidal currents were often strong (> 1 m/s). The Swellies is a topographically constricted region that acts as a potential barrier to connectivity between the mussel beds located in the south and the north of the Menai Strait. Harvey (1968) made the same observations with drifters released at the south entrance of the Menai Strait. Despite the SW residual current, particles can travel north in the Menai Strait over one week. This phenomenon could be caused by strong southwest winds that reverse the surface flow (Simpson 1971) or by the transverse flow on the ebb tide trapping particles close to the banks of the channel (Robins et al. 2012). The results of this study suggested that approximately 10% of particles released from the Bangor mussel bed reached both the north and south ends of the Menai Strait. These results are correlated somewhat with Harvey (1968), in which approximately 10% and 3% of drifters released from Bangor were found at both south and north ends.

Particles released during neap and spring tide showed no significant difference in their dispersal after one week, although the spring tidal averaged current was 10% larger than the neap. However, in the northern section of the channel, the spring tidal averaged current direction differed markedly from that during neap tide release (Fig. 14). This difference caused the particles during spring tide to remain in this area by pushing them towards the coast. Larvae were simulated to travel further south when released during neap tides (Fig. 10), despite stronger spring flows. However, the ebb tidal averaged current was higher during neap than spring tides at the southern end of the channel (Fig. 14). A previous study performed by Campbell et al. (1998) showed that the ebb flow southwards was 10 to 15% stronger than the flood flow northwards in the southern channel. The results above confirmed this when 65% of the particles found in the southern part of the Menai Strait came from a release during neap tides. For the particles released from the Bangor mussel bed

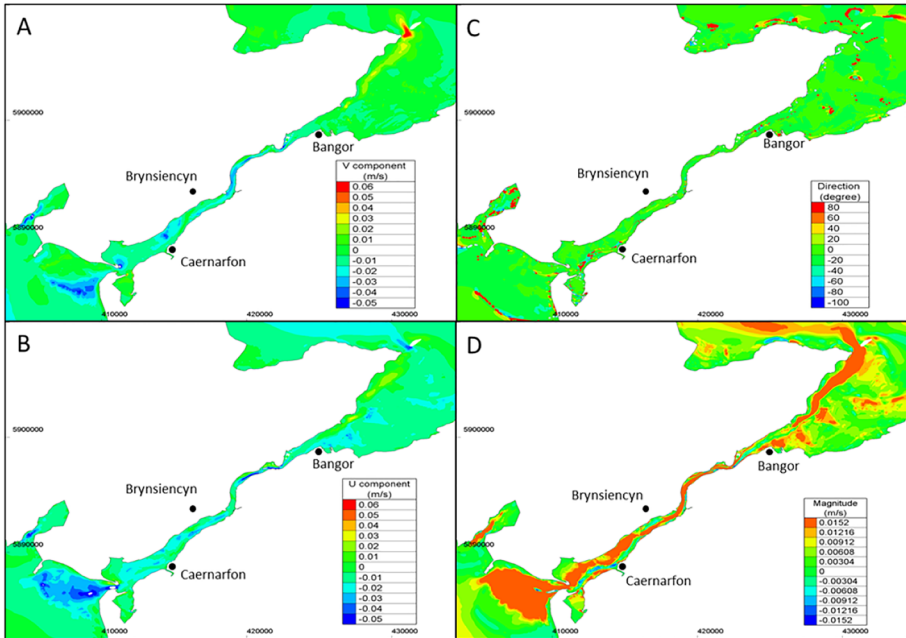


**Fig. 14** Difference of the tidal averaged currents between simulations starting during spring tide and simulations starting during neap tide. Results present the difference for (A) V component in m/s, (B) U component in m/s, (C) direction in degrees and (D) magnitude in m/s. Warm colours (red to yellow) show a positive difference when spring is higher than neap. Green colours show when both tidal averaged currents are equal. Cold colours (light to dark blue) show when neap is higher than spring

during the flood tide, they had more chance of exiting the channel from the north than the south. The same predictions were made for simulations releasing particles at HW and LW.

### Conclusion

Blue mussel *Mytilus edulis* shellfisheries rely on wild spat collection; however, wild spat distributions depend on the timing of larval spawning within the connected metapopulation and the larval dispersal potential that is contingent on interacting biophysical parameters. Being able to predict the spawning events could potentially help mussel producers to plan their mussel seed harvesting strategy (e.g. between three and six weeks after spawning) and hence save costs. This study highlighted that (1) spawning events occurred several times during spring and summer 2018, which improves our knowledge of the timing and frequency of the blue mussel in the northern part of the Irish Sea; (2) based on model simulations parameterised with the above spawning information from the fieldwork, it is possible to predict the likely dispersal patterns of mussel larvae from the Menai Strait. We did this for the year 2018, showing a majority southwards dispersal through the channel (driven by tidal asymmetric and therefore an expected pattern during other years). As mussels from commercial beds in the Menai Strait seem to disperse away from their native bed, further investigations should be carried out to study the contribution to a wider population within the northern Irish Sea

over a larval period of several weeks. This fieldwork and modelling results combined give further insight for shellfisheries aquaculture to collect wild spat and open a possibility to use new methods of harvest (like offshore ropes, for example, instead of actual dredging) to minimise the environmental impact of human activities on coastal habitat.

**Acknowledgements** The authors wish to acknowledge KESS2 for their financial support, but also Extramussels Limited for their financial support and constructive knowledge on mussel aquaculture in North Wales. Oceanographic data was provided through the SEACAMS project ([www.seacams.ac.uk](http://www.seacams.ac.uk)), funded by the Welsh Government, the Higher Education Funding Council for Wales, the Welsh European Funding Office, and the European Regional Development Fund (ERDF) Convergence Programme. The authors were also supported by the ERDF Interreg Ireland-Wales projects Bluefish (Grant Agreement No. 80991) and ECOSTRUCTURE (<http://www.ecostructureproject.eu/>) and the ERDF/WEFO Smart Efficient Energy Centre (SEEC) at Bangor University. The model simulations were conducted on the Supercomputing-Wales high-performance computing ([www.supercomputing.wales](http://www.supercomputing.wales)) system (a collaboration between Welsh universities and the Welsh Government), supported by Ade Fewings and Aaron Owen.

**Author contribution** Jonathan Demmer, Peter Robins and Simon Neill designed the model and the computational framework and performed the simulations. Trevor Jones and Shelagh Malham provided data and knowledge on mussel larvae to design the experiment and define the areas of interest. Olga Andres provided data on sea surface temperature. Jonathan Demmer analysed the data and wrote the article. All authors provided critical feedback and helped shape the research, analysis and article.

**Funding** This study was funded by KESS2, SEEC and Extramussels Limited.

**Data availability** The datasets generated during and analysed during the current study are available from the corresponding author on reasonable request.

**Code availability** Not applicable.

## Declarations

**Ethics approval** Not applicable.

**Conflict of interest** The authors declare no competing interests.

**Open Access** This article is licensed under a Creative Commons Attribution 4.0 International License, which permits use, sharing, adaptation, distribution and reproduction in any medium or format, as long as you give appropriate credit to the original author(s) and the source, provide a link to the Creative Commons licence, and indicate if changes were made. The images or other third party material in this article are included in the article's Creative Commons licence, unless indicated otherwise in a credit line to the material. If material is not included in the article's Creative Commons licence and your intended use is not permitted by statutory regulation or exceeds the permitted use, you will need to obtain permission directly from the copyright holder. To view a copy of this licence, visit <http://creativecommons.org/licenses/by/4.0/>.

## References

- Battle HI (1931) Rhythmic sexual maturity and spawning of certain bivalve. *Cont Canadian Biol Fish: Being Stud Biol Stations Canada* 7 (257)
- Becker BJ, Levin LA, Fodrie FJ, McMillan PA (2007) Complex larval connectivity patterns among marine invertebrate populations. *Ecology* 104:3267–3272
- Bergstrom P, Lindegarh M (2016) Environmental influence on mussel (*Mytilus edulis*) growth – a quantile regression approach. *Estuar Coast Shelf Sci* 171:123–132
- Campbell AR, Simpson JH, Allen GL (1998) The dynamical balance of flow in the Menai Strait. *Estuar Coast Shelf Sci* 46:449–455



- Cefas (2012) Aquaculture statistics for the UK, with a focus on England and Wales. *Cefas Weymouth*.
- Chipperfield PNJ (1953) Observations on the breeding and settlement of *Mytilus edulis* (L.) in British waters. *J Marine Biol Assoc UK* 32:449–476
- Commito JA, Commito AE, Platt RV, Grupe BM, Dow Piniak WE, Gownaris NJ, Reeves KA, Vissicelli AM (2014) Recruitment facilitation and spatial pattern formation in soft-bottom mussel beds. *Ecosphere* 5(12):160
- Coscia I, Robines PE, Porter JS, Malham SK, Ironside JE (2013) Modelled larval dispersal and measured gene flow: seascape genetics of the common cockle *Cerastoderma edule* in the southern Irish Sea. *Conserv Genet* 14:451–466
- Dauhajre DP, McWilliams JC, Renault L (2019) Nearshore Lagrangian connectivity: submesoscale influence and resolution sensitivity. *J Geophys Res* 124:5180–5204
- Dare PJ, Edwards DB (1975) seasonal changes in flesh weight and biogeochemical composition of mussels (*Mytilus edulis* L.) in the Conwy estuary, North Wales. *J Exp Mar Biol Ecol* 18:89–97
- Davies AM, Robins PE (2017) Residual flow, bedforms and sediment transport in a tidal channel modelled with variable bed roughness. *Geomorphology* 295:855–872
- Demmer J (2020) Simulating the temporal and spatial variability of north Wales mussel populations. PhD thesis Bangor University, Wales
- Demmer J, Robins P, Malham S, Lewis M, Owen A, Jones T, Neill S (2022) The role of wind in controlling the connectivity of blue mussels (*Mytilus edulis* L.) populations. *Movement Ecol* 10 (3)
- De Vooy CGN (1999) Numbers of larvae and primary plantigrades of the mussel *Mytilus edulis* in the western Dutch Wadden Sea. *J Sea Res* 41:189–201
- Doherty SD, Brophy D, Gosling E (2009) Synchronous reproduction may facilitate introgression in a hybrid mussel (*Mytilus*) population. *J Exp Mar Biol Ecol* 378:1–7
- Duinker A, Haland L, Hovgaard P, Mortensen S (2008) Gonad development and spawning in one and two-year-old mussels (*Mytilus edulis*) from Western Norway. *J Marine Biol Assoc UK* 88:1465–1473
- Ekokotu PA, Olele NF (2014) Cycle of gonad maturation, condition index and spawning of *ClarotesLaticeos* (claroteidae) in the lower river Niger. *Int J Fish Aquat Stud* 1(6):144–150
- Ewins PA, Spencer CP (1967) The annual cycle of nutrients in the Menai Straits. *J Mar Biol Assoc UK* 47:533–542
- Famme P, Riisgard HU, Jorgensen CB (1986) On direct measurement of pumping rates in the mussel *Mytilus edulis*. *Mar Biol* 92:323–327
- Fernandez A, Grienke U, Soler-Vila A, Guiheneuf F, Stengel DB, Tasdemir D (2015) Seasonal and geographical variations on the biochemical composition of the blue mussel (*Mytilus edulis* L.) from Ireland. *Food Chem* 177:43–52
- Filgueira R, Comeau LA, Landry T, Grant J, Guyondet T, Mallet A (2013) Bivalve condition index as an indicator of aquaculture intensity: a meta-analysis. *Ecol Ind* 25:215–229
- Gardner JPA, Skibinski DOF (1990) Genotype-dependent fecundity and temporal variation of spawning in hybrid mussel (*Mytilus*) populations. *Mar Biol* 105:153–162
- Gowen RJ, Stewart BW, Mills DK, Elliott P (1995) Regional differences I stratification and its effect on phytoplankton production and biomass in the north western Irish Sea. *J Plankton Res* 17(4):753–769
- Gowen RJ, Stewart BW (2005) The Irish Sea: nutrients status and phytoplankton. *J Sea Res* 54(1):36–50
- Harnett M, Berry A, Tully O, Dabrowski T (2007) Investigations into the transport and pathways of scallop larvae – the use of numerical models for managing fish stocks. *J Environ Monit* 9:403–410
- Harvey JG (1968) The flow of water through the Menai Straits. *Geophys J Roy Astron Soc* 15:517–528
- Hennebicq R, Fabra G, Pellerin C, Marcotte I, Myrand B, Tremblay R (2013) The effect of spawning of cultured mussels (*Mytilus edulis*) on mechanical properties, chemical and biochemical composition of byssal threads. *Aquaculture* 410:11–17
- Holt JT, Proctor R (2003) The role of advection in determining the temperature structure of the Irish Sea. *J Phys Oceanogr* 33:2288–2306
- Horvath T, Crane L (2010) Hydrodynamics forces affect larval zebra mussel (*Dreissenapolyomorpha*) mortality in a laboratory setting. *Aquat Invasions* 5(4):379–385
- Howarth MJ (2005) Hydrography of the Irish Sea. Tech. rep., SEA6 Technical report, Department of Trade and Industry offshore energy Strategic Assessment programme, UK
- Irisarri J, Fernandez-Reiriz M-J, Labarta U (2015) Temporal and spatial variations in proximate composition and condition index of mussels *Mytilusgalloprovincialis* cultured in suspension in a shellfish farm. *Aquaculture* 435:207–216

- James MK, Polton JA, Brereton AR, Howell KL, Nimmo-Smith WAM, Knights AM (2019) Reverse engineering field-derived vertical distribution profiles to infer larval swimming behaviours. *Proc Natl Acad Sci USA* 116(24):11818–11823
- Kratzer S, Buchan S, Bowers DG (2003) Testing long-term trends in turbidity in the Menai Strait, North Wales. *Estuar Coast Shelf Sci* 56:221–226
- Li Y, Qin JG, Li X, Benkendorff K (2009) Monthly variation of condition index, energy reserves and anti-bacterial activity in Pacific oysters, *CrassostreasGigas*, in Stansbury (South Australia). *Aquaculture* 286(1):64–71
- Massapina C, Joaquim S, Devauchelle N (1999) Oocyte and embryo quality in *Crassostreagigas* (Portuguese strain) during a spawning period in Algarve. *South Portugal Aquatic Living Res* 12(5):327–333
- Nanninga GB, Berumen ML (2014) The role of individual variation in marine larval dispersal. *Front Mar Sci* 1(71):1–17
- Newell RIE, Hilbish TJ, Koehn RK, Newell CJ (1982) Temporal variation in the reproductive cycle of *Mytilus edulis* L (Bivalvia, Mytilidae) from localities on the east coast of the United States. *Biol Bull* 162(3):229–310
- North EW, Schlag Z, Hood RR, Li M, Zhong L, Gross T, Kennedy VS (2008) Vertical swimming behaviour influence the dispersal of simulated oyster larvae in a coupled particle-tracking and hydrodynamic model of Chesapeake Bay. *Mar Ecol Prog Ser* 359:99–115
- Pearson RV, Barber RW (1998) Modelling depth-integrated coastal pollution using a Lagrangian particle technique. *Trans Ecol Environ*(17)
- Ompi M, Svane I (2018) Comparing spawning, larval development, and recruitment of four mussel species (Bivalvia: Mytiidae) from South Australia. *Aquacult Aquarium Conserv Legis* 11(3):576–588
- Pernet F, Tremblay R, Bourget E (2003) Settlement success, spatial pattern and behaviour of mussel larvae *Mytilus* spp. In experimental ‘down-welling’ systems of varying velocity and turbulence. *Mar Ecol Prog Ser* 260:125–140
- Proctor R, Flather RA, Elliott AJ (1994) Modelling tides and surface drift in the Arabian Gulf – applications to the gulf oil spill. *Cont Shelf Res* 14(5):531–545
- Ram JL, Fong PP, Garton DW (1996) Physiological aspects of zebra mussels reproduction: maturation, spawning and fertilization. *Am Zool* 36(3):326–338
- Reaugh KE (2006) Recruitment patterns and processes and the connectivity of rocky shores in southern Africa. PhD thesis, University of Cape Town, South Africa
- Rhörs J, Christensen KH, Vikebo F, Sundby S, Saetra O, Brostrom G (2014) Wave induced transport and vertical mixing of pelagic eggs and larvae. *Limnol Oceanogr* 59(4):1213–1227
- Richardson L (2016) UK sea fisheries statistics 2015. Marine Management Organisation
- Rippeth TR, Williams E, Simpson JH (2001) Reynolds stress and turbulent energy production in a tidal channel. *J Phys Oceanogr* 32:1242–1251
- Robins PE, Neill S, GimenezNoya J (2012) A numerical study of marine larval dispersal in the presence of an axial convergent front. *Estuarine, Coast Shelf Sci* 100:172–185
- Ross ON, Sharples J (2004) Recipe for 1-D Lagrangian particle tracking models in space-varying diffusivity. *Limnol Oceanogr* 2(9):289–302
- Sahin C, Duzgunes E, Okumus I (2006) Seasonal variations in condition index and gonad development of the introduced blood cockle *Anadara inaequivalvis* (Bruguiere, 1789) in the Southeastern Black Sea coast. *Turk J Fish Aquat Sci* 6:155–163
- Seed R (1969) The ecology of *Mytilus edulis* L. (lamellibranchiate) on exposed rocky shore. *Oecologia* 3:277–316
- Sheaves M (2009) Consequences of ecological connectivity: the coastal ecosystem mosaic. *Mar Ecol Prog Series* 391:107–115
- Simpson JH (1971) Density stratification and microstructure in the western Irish Sea. *Deep-Sea Res Oceanogr Abstr* 18(3):309–319
- Simpson JH, Bex B, Gascoigne J, Saurel C (2007) The interaction of tidal advection, diffusion and mussel filtration in a tidal channel. *J Mar Syst* 68(3):556–568
- Slabyj BM, Creamer DL, True RH (1978) Seasonal effect on yield, proximate composition, and quality of blue mussel, *Mytilus edulis*, meats obtained from cultivated and natural stock. *Mar Fish Rev* 40(8):18–23
- Smaal AC, van Stralen MR (1990) Average growth and condition of mussels as a function of food source. *Hydrobiologia* 195:179–188
- Sprung M (1984) Physiological energetics of mussel larvae (*Mytilus edulis*). I. Shell growth and biomass. *Mar Ecol Prog Ser* 17:283–293

- Troost K, Veldhuizen R, Stamhuis EJ, Wolff WJ (2008) Can bivalve veligers escape feeding currents of adult bivalves? *J Exp Mar Biol Ecol* 358(2):185–196
- Van der Schatte AO, Jones L, Le Vay L, Christie M, Wilson J, Malham SK (2018) A global review of the ecosystem services provided by bivalve aquaculture. *Rev Aquacult* 1–23
- Villaret C, Hervouet JM, Kopmann R, Merkel U, Davies AG (2013) Morphodynamic modelling using the TELEMAC finite-element system. *Comput Geosci* 53:105–113
- Weidberg N, Porri F, Von der Meden CEO, Jackson JM, Goschen W, McQuaid CD (2015) Mechanisms of nearshore retention and offshore export of mussel larvae over the Alghus Bank. *J Mar Syst* 144:70–80

**Publisher's note** Springer Nature remains neutral with regard to jurisdictional claims in published maps and institutional affiliations.